J. Earth Syst. Sci. (2019)128 222
https://doi.org/10.1007/s12040-019-1250-2

Revisiting the boundary between the Lower and Upper Vindhyan, Son valley, India

Sabyasachi Mandal[1], Adrita Choudhuri[2], Indrani Mondal[1], Subir Sarkar[1,*], Partha Pratim Chakraborty[3] and Santanu Banerjee[4]

[1]*Department of Geological Sciences, Jadavpur University, Kolkata 700 032, India.*
[2]*Department of Earth Sciences, Indian Institute of Science Education and Research, Kolkata, Mohanpur, West Bengal 741 246, India.*
[3]*Department of Geology, University of Delhi, New Delhi 110 007, India.*
[4]*Department of Earth Sciences, Indian Institute of Technology Bombay, Mumbai 400 076, India.*
**Corresponding author. e-mail: jugeoss@gmail.com*

MS received 3 February 2019; revised 12 June 2019; accepted 13 June 2019

The placement of the boundary between the Lower and the Upper Vindhyan in the Son valley, an unconformity, has long been at the centre of a raging debate. At the Bundelkhand sector, it is placed between the Rohtas Limestone and the Sasaram Sandstone (Lower Quartzite). On the other hand, in the Son valley sector, it is placed between the Bhagwar Shale and the Kaimur Formation. The recent study reveals the existence of ca. 12 m thick sandstone between the Bhagwar Shale and Rohtas Limestone, traced over 150 km in the Son valley sector. Based on in-depth facies constituents and facies tracts, this sandstone is an exact equivalent of the Sasaram Sandstone in the Bundelkhand sector. Its base is strongly erosional and limestone and chert clasts derived from the underlying Rohtas Limestone are abundantly present at the basal part of the sandstone and the unconformity between the Upper and Lower Vindhyan are likely to be present in between.

Keywords. Lower Vindhyan; Upper Vindhyan; unconformable boundary; transgressive lag; persistent sandstone horizon; subtidal deposit.

1. Introduction

The Palaeo to the Neoproterozoic Vindhyan Supergroup, the largest 'Purana' basin in India and the world's second-largest Proterozoic basin, is one of the most well studied and focused Proterozoic successions in India (figure 1a; Auden 1933; Banerjee 1974; Sastry and Moitry 1984; Bhattacharyya 1996; Rai *et al.* 1997; Seilacher *et al.* 1998; Bose *et al.* 2001, 2015; Rasmussen *et al.* 2002; Ray *et al.* 2002; Sarkar *et al.* 2002a, 2004, 2006, 2014; Banerjee *et al.* 2006; Malone *et al.* 2008; Bengtson *et al.* 2009, 2017; Kumar and Sharma 2011; Chakraborty *et al.* 2012; Gopalan *et al.* 2013; Tripathy and Singh 2015; Bickford *et al.* 2017; Gilleaudeau *et al.* 2018; Mishra *et al.* 2018; Sallstedt *et al.* 2018). The Vindhyan basin, exposed in the eastern part of central India can be divided into the Bundelkhand sector and the Son valley sector (figure 1a, Chakraborty 2006; Chakraborty *et al.* 2010). The basin-wide unconformity divides the Vindhyan succession into two parts, the Lower Vindhyan/ Semri Group and the Upper Vindhyan (figures 1 and 2). However, the exact stratigraphic position of the unconformity is still controversial. From previous studies carried out in the Bundelkhand

Published online: 10 August 2019

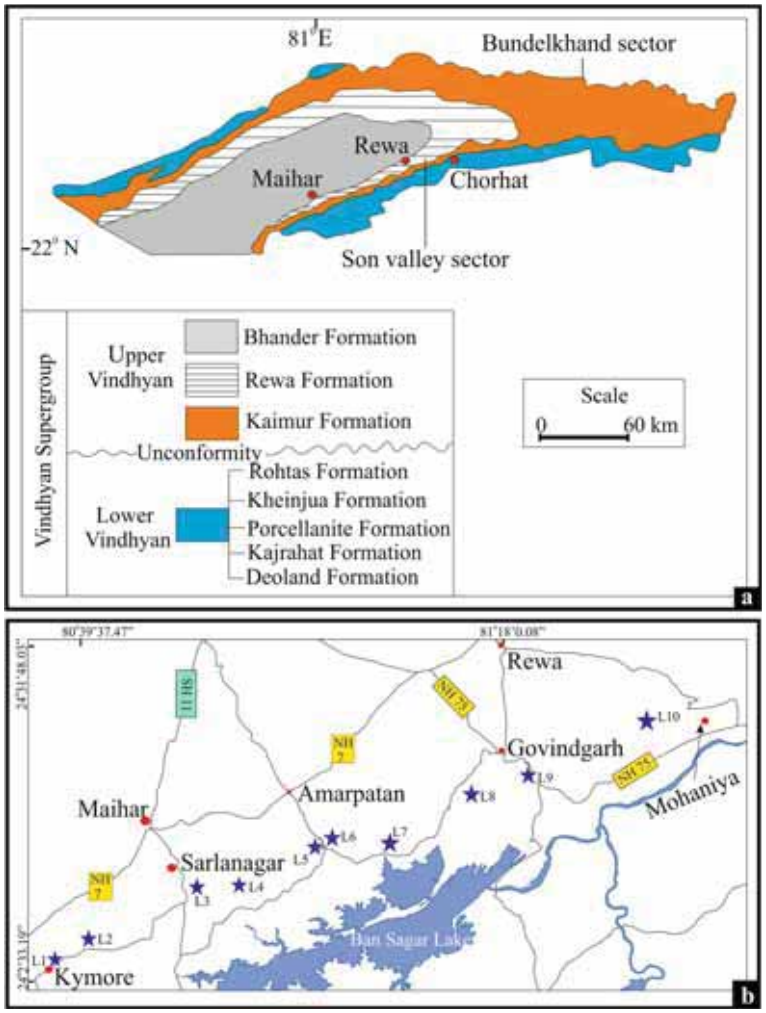

Figure 1. Lithological map of the Vindhyan Supergroup and stratigraphy of the Vindhyan Supergroup, central India (**a**). The location map of the studied area (marked by stars) in the Son valley sector, central India (**b**).

sector, the unconformity lying between the Lower and Upper Vindhyan has been considered above the Rohtas Limestone (the topmost succession of the Lower Vindhyan Group) and below the Sasaram Sandstone (equivalent to Lower Quartzite of the Kaimur Formation; Chakraborty 2006; figure 2). In contrast to this, most of the previous studies in the Son valley sector noted that the top part of the Rohtas Limestone gradually passes upward into the Bhagwar Shale which is composed of sand–silt alternations with a substantial amount of the volcanic input (figure 2; Banerjee 1974; Sastry and Moitry 1984; Chakraborty and Chaudhuri 1990; Bhattacharyya 1996; Chakraborty 2006; Kumar and Sharma 2011) and the unconformity between the Lower and Upper Vindhyan lies above this shale (figure 2). A claim has also been made that the arkosic/pebbly sandstone of the Sasaram Sandstone (also known as the Lower Quartzite) observed above the unconformity in the Bundelkhand sector is absent in the Son valley sector (Chakraborty 2006).

Recent fieldwork in the Son valley sector along ∼150 km stretch from Mohaniyain in the east (24°25′34.06″N, 81°40′8.86″E) to Kymore (24°3′36.78″N, 80°36′31.53″E) in the west (figure 1b) reveals the presence of a sandstone having a maximum thickness of ∼12 m immediately above the Rohtas Limestone with a sharp, undulating and erosional contact in between (figure 3). A thin (ca. 10 cm), laterally persistent and sheet-like coarse-grained layer with chertified limestone clasts demarcates the erosional contact between the Rohtas Limestone and the sandstone (figures 2 and 4a). So far the sandstone had not been described and a detailed sedimentalogical study of this sandstone is non-existent. Possibly, this is the reason why most of the previous workers

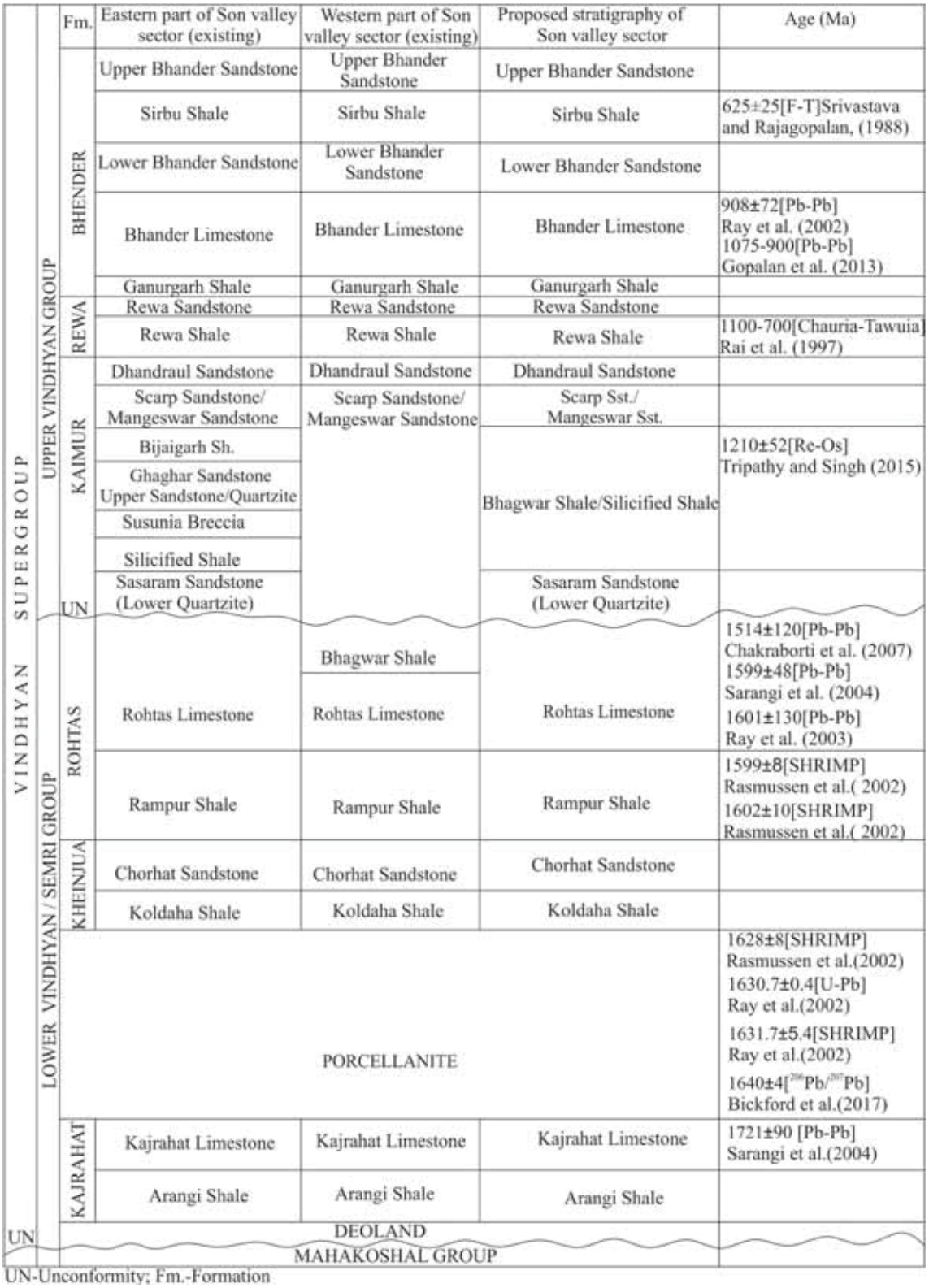

Figure 2. Stratigraphy of the Vindhyan Supergroup, Son valley (modified after Auden 1933; Banerjee 1974; Rao and Neelakantam 1978; Sastry and Moitra 1984; Bhattacharyya 1996; Chakraborty 2006; Chakraborty *et al.* 2010; Kumar and Sharma 2011).

considered the Bhagwar Shale within the Lower Vindhyan/Semri Group and found that the unconformity is placed above it (Banerjee 1974; Rao and Neelakantam 1978; Sastry and Moitry 1984; Bhattacharyya 1996; Chakraborty 2006; Valdiya 2010; Kumar and Sharma 2011).

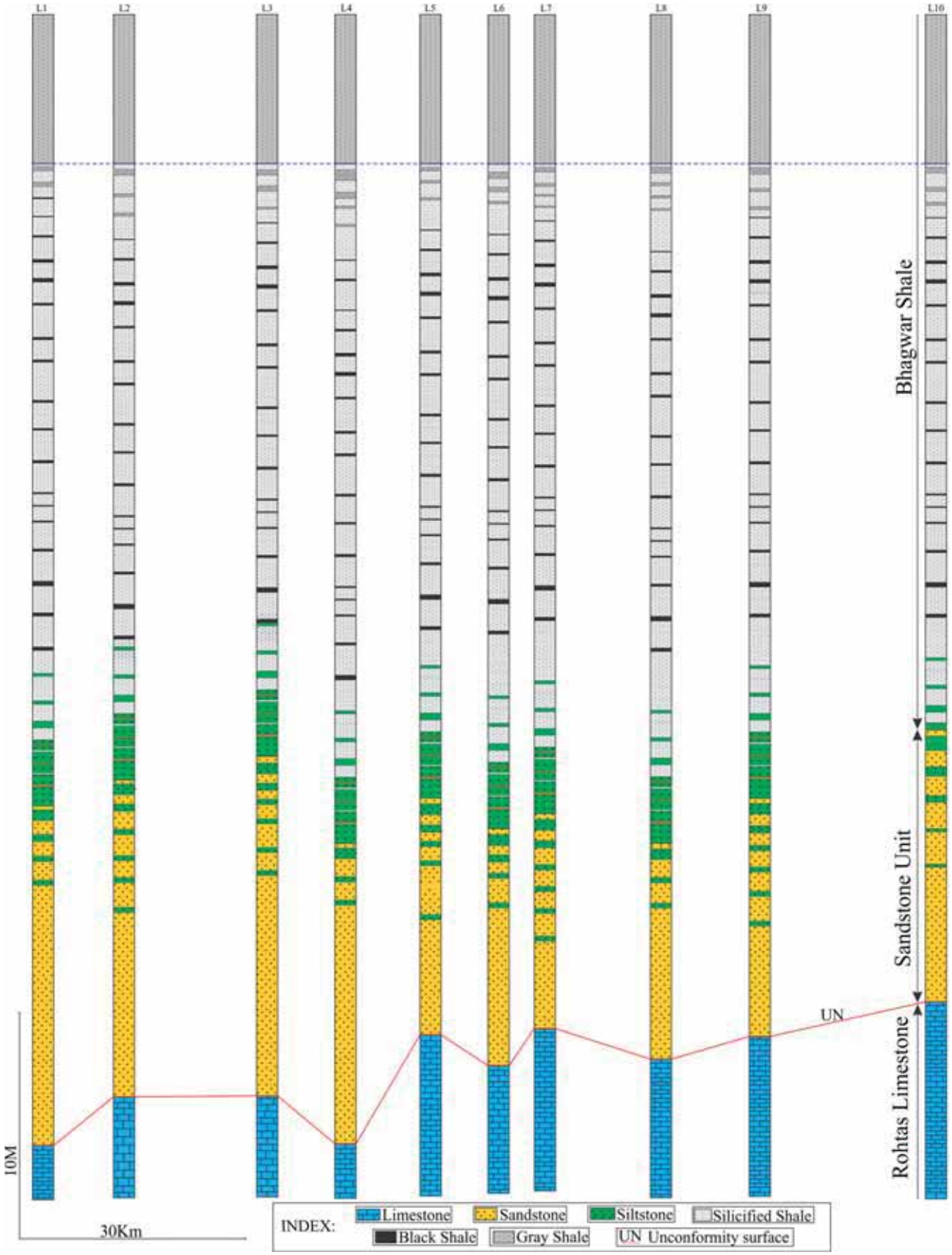

Figure 3. Stratigraphic sections across the boundary between the Lower and Upper Vindhyan along the studied stretch (marked in figure 1b). Note the unconformable relationship between the Rohtas Limestone and the overlying sandstone unit. Also note the gradational relationship between the sandstone and the overlying Bhagwar Shale.

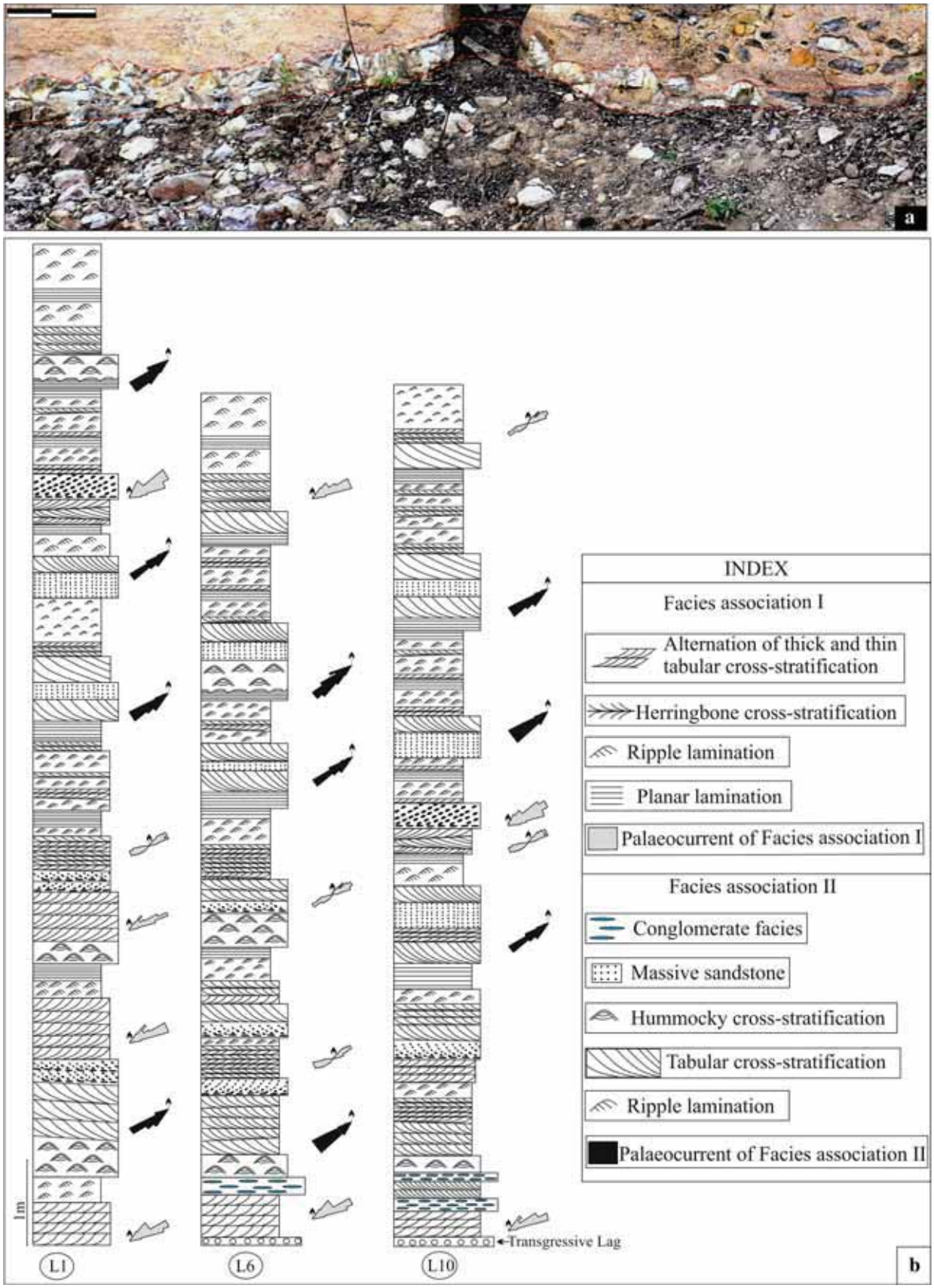

Figure 4. Transgressive lag present at the basal part of the sandstone (marked by dotted lines, bar length 20 cm) (**a**). Distribution of the facies associations along with palaeocurrent directions of two facies associations in three best-exposed localities (**b**).

The goal of the present paper is to revisit the boundary between the Lower and Upper Vindhyan in the Son valley sector and also to record the nature of this contact with the help of a detailed sedimentary facies analysis of this sandstone, hitherto undescribed.

2. Geological background

The Vindhyan basin, developed during the Palaeo to the Neoproterozoic time (Bose *et al.* 2001; Chakraborty *et al.* 2010), rests unconformably on the Aravalli craton, the Bundelkhand granitic gneiss and the Mahakoshal group of rocks. The Vindhyan rocks are distributed over $\sim$1,00,000 km^2. The Vindhyan sediments are generally unmetamorphosed and only mildly deformed. The geophysical investigation has suggested the presence of the E–W trending faults that initiated the formation of the Vindhyan basin (Naqvi and Rogers 1987). The rifting was accompanied by a dextral shear which created some NW–SE elongated sub-basins where the sedimentation took place (Bose *et al.* 1997, 2001). As a result, strike-wise variations in both thicknesses of the constituting facies and sediment character changes are rapid in the Lower Vindhyan/Semri Group (Bose *et al.* 2001). Contrastingly, the Upper Vindhyan Group is laterally persistent, likely to be deposited in a sag basin (Chanda and Bhattacharyya 1982; Bose *et al.* 2001; Sarkar *et al.* 2002b). The beds are much steeper in the lower part compared to that of the upper part of the Vindhyan succession.

The Vindhyan sediments are divided into three outcrop sectors, namely, the Bundelkhand sector, Son valley sector and Rajasthan sector (Chakraborty 2006; Chakraborty *et al.* 2010). The Bundelkhand and Rajasthan sectors are dominated by carbonate sediments; the sediments in the Son valley sector are represented by both siliciclastic and carbonate sediments in nearly equal volume (Chakraborty 2006; Chakraborty *et al.* 2010). The Son valley Vindhyan has a maximum thickness of 4.5 km. They are constituted by two groups, the Lower Vindhyan/Semri Group and the Upper Vindhyan Group separated by a basin-wide unconformity (figures 1a and 2; Kumar 1978a, b; McMenamin *et al.* 1983; Chakraborty and Bose 1992a, b; Chakraborty 1993; Bose *et al.* 2001; Schieber *et al.* 2007; Paikaray *et al.* 2008; Pati *et al.* 2008; Raza *et al.* 2010; Sallstedt *et al.* 2018). Five Formations are present (Deoland, Kajrahat, Porcellanite, Kheinjua and Rohtas) within the Lower Vindhyan Group while there are three Formations (Kaimur, Rewa and Bhander) present within the Upper Vindhyan Group (Kumar 1978a, b; McMenamin *et al.* 1983; Chakraborty and Bose 1992a, b; Chakraborty 1993; Bose *et al.* 2001; Schieber *et al.* 2007; Paikaray *et al.* 2008; Pati *et al.* 2008; Raza *et al.* 2010; Sallstedt *et al.* 2018). The age of the Vindhyan Supergroup ranges from 1721 to 650 ma (Chakraborty *et al.* 2010 and references there in; Gopalan *et al.* 2013; Tripathy and Singh 2015; Bickford *et al.* 2017). Dominant lithologies of the Supergroup are mature sandstone, shale, carbonate and conglomerate, mostly intra-formational. The dominance of a shallow marine depositional regime has been considered mostly (Singh 1973; Banerjee 1974; Chanda and Bhattacharyya 1982; Prasad and Verma 1991) with a range of variation from the barrier bar–lagoon, tidal and beach to a relatively deeper part of the shelf (Chakraborty and Bose 1992a, b; Chakraborty 1995; Bose *et al.* 2001; Sarkar *et al.* 1996, 2002a, b). On the other hand, subordinate amounts of fluvial and aeolian deposits have also been reported from the supergroup (Bhattacharyya and Morad 1993; Bose and Chakraborty 1994; Bose *et al.* 1999; Chakraborty and Chakraborty 2001).

3. Stratigraphic problem

The Bhagwar Shale is well exposed in parts of the Son valley sector (figure 3). The Bhagwar Shale composed of sand–silt alternations with a substantial amount of the volcanic input (Chakraborty 2006; figure 3). The shale is well exposed along the studied stretch (figure 1b). A persistent sandstone layer is present below the shale (figure 3). The upper contact of the sandstone with the Bhagwar Shale is gradational while the lower contact of the sandstone is sharp and undulatory with the underlying Rohtas Limestone (figure 3). The contact of the Bhagwar Shale is also gradational with the overlying Kaimur Formation. The colour of the shale varies from grey to dark grey, even black at places, both vertically as well as laterally. The sand/silt stringers present within the shale are laterally continuous. Some laterally persistent sand layers with sole features at their bases are present within the shale. Very fine-grained tuff layers are also present within the Bhagwar Shale (see figure in Chakraborty *et al.* 1996). As discussed, the sandstone below the Bhagwar Shale is directly overlying the Rohtas Limestone (figures 3 and 4a) and here lies the problem of placing the boundary between the Lower and Upper Vindhyan in this

sector. So far, in most of the studies, the boundary has been demarcated above the Bhagwar Shale which shows a gradational boundary with the overlying Mangeswar/Scrap Sandstone of Kaimur Formation. However, the sandstone lying below the Bhagwar Shale has not been reported earlier in the Son valley sector, and hence, demands a detailed study before considering the contact between the Lower and the Upper Vindhyan.

4. Facies analysis of the sandstone present immediately above the Rohtas Limestone

Deposition of the Semri/Lower Vindhyan Group ends with a ca. 110 m thick Rohtas Limestone (topmost part of the Rohtas Formation). The upper part of the Rohtas Limestone is chertified in many places (figure 4a). The Rohtas Limestone in the Son valley sector is overlain by ca. 12 m thick sandstone unit (figures 3 and 4b). The boundary between the Rohtas Limestone and the overlying sandstone is sharp, erosional and demarcated by a thin (∼10 cm) sheet-like unit containing pebbles of chertified limestone (av. clast size 5 cm) at several places in the study area (figure 4a). Possibly, these pebbles are derived from the upper part of the chertified Rohtas Limestone.

This sheet-like pebble-bearing unit is followed upward by a laterally persistent sandstone unit (max. thickness 12 m) along with an ∼150 km east–west stretch of the study area (figure 1b). The overall grain size of this sandstone varies from coarse to fine sand. Considering the primary sedimentary structures, sediment composition and bed geometry, the sandstone can be subdivided into two facies associations: (a) Facies association I and (b) Facies association II (figure 4b). The constituting facies of Facies association I is in general of fine to medium size sandstone and also rich in mud compared to that of Facies association II. As mentioned earlier, the details regarding this sandstone unit are not available in the literature, so we thought it is a pre-requisite to discuss this sandstone in detail before finalising the boundary between the Lower and the Upper Vindhyan in the Son valley. The following are the detailed description and interpretations for each facies association of the sandstone.

4.1 *Facies association I*

Facies association I is distinctly different from the Facies association II with respect to the grain size (varying from medium to fine sand) and mud content. This Facies association I is dominantly cross-stratified in nature and consists of the following four facies.

4.1.1 *Alternation of thick and thin tabular cross-stratified sandstone facies*

This facies comprises medium- to fine-grained sandstone exhibiting unidirectional cross-stratification. It is present at the basal part of the sandstone and lies exactly on top of the basal thin and sheet-like pebble-bearing unit (marked by dotted lines in figure 4a). The average thickness of the facies is 15 cm. Internally, the cross-stratifications are characterised by an alternation of thick and thin planar tabular cross-strata (figure 5a), the foreset bundles are separated by mudstone partings (figure 5a). The thickness of the individual foreset varies between 0.5 and 3.2 cm, whereas the mudstone laminae are a few sub-millimetres thick. The thickness measurement of cross-set bundles reveals a nearly symmetrical pattern of cyclicity (figure 5b). A maximum of 28 laminae occurs between two successive peaks of the thick laminae (figure 4b). Usually, the foreset dip decreases from the highest peak to the trough of the sinuous curve. The dips of the cross-sets decrease down current from ca. 30° to ca. 15° and laterally pass over into compound cross-stratification at times (marked in figure 5c; Rouse 1961; Bose *et al.* 1997). Some of the foresets are defined by mud clasts (figure 5d). At places, thick mud drapes (up to 2 cm) occur within the cross-lamina set (figure 5c). Small-scale cross-lamina (ca. 3 cm thick) dipping oppositely is occasionally present within the larger foreset of the cross-bedding (marked in figure 5c).

4.1.2 *Herringbone cross-stratified sandstone facies*

Two sets of oppositely dipping cross-strata separated by a gently inclined, planar erosional surface constituting a herringbone pattern is another facies of this association (figure 5e). The average thickness of this facies is 30 cm. The orientation of the herringbone cross-strata shows a distinct bipolar and bimodal palaeocurrent direction all over the studied stretch (figure 5f). Double mud drape is a characteristic feature of the foresets (figure 5g). Mud clasts

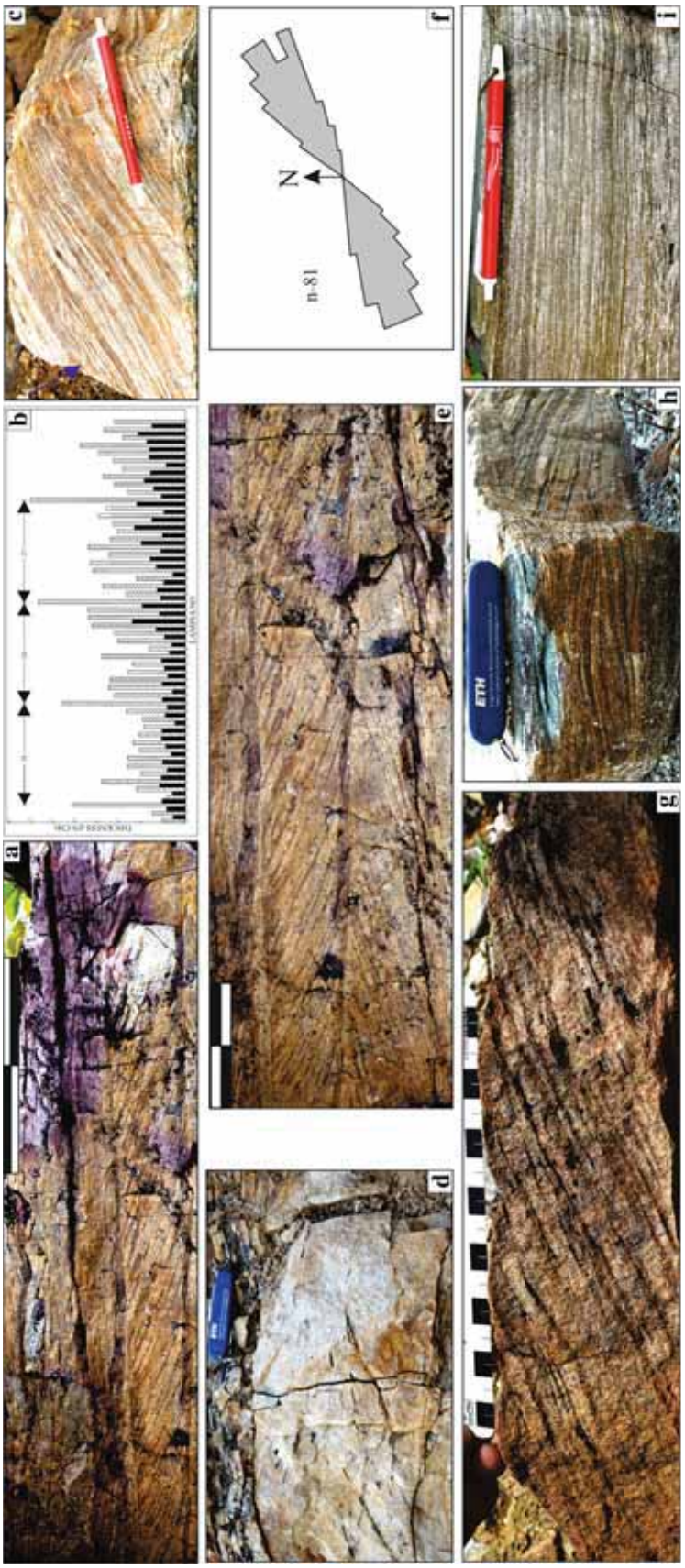

Figure 5. Facies association I of the studied sandstone; alternation of thick and thin tabular cross-stratification within the tabular cross-stratified sandstone facies (**a**, bar length 10 cm). Note the cyclic thickness variations within the facies (**b**). Thick mud drape within the cross-stratification (**c**). Note the oppositely oriented smaller cross-sets within the larger set (c, marked by blue arrow; pen length 15 cm). Mud clast alignment along cross-stratification (**d**, length of knife 8 cm). Herringbone arrangement of cross-stratification (**e**, bar length 15 cm). The rose diagram with bimodal bipolar orientation (**f**). Cross-bedding with double mud drape (**g**, scale length 15 cm). Sigmoidal cross-stratification and thick mud drape within the ripple-laminated facies (**h**, length of knife 8 cm). Planar lamination with intermittent mud laminae (**i**, pen length 15 cm).

are present along the boundary between two differently oriented sets of cross-stratification at places (figure 5d).

4.1.3 *Small-scale ripple-laminated sandstone facies*

This facies is characterised by small-scale ripple-laminated sandstone and is commonly associated with the facies 4.1.1 (figure 5h). Mud is present at the trough of some of the ripples (figure 5h). The maximum thickness of the ripple foreset is 5 cm. Thick mud partings occur at the ripple set boundaries (figure 5h). Ripple cross-lamina exhibits sigmoidal patterns at places (figure 5h).

4.1.4 *Planar-laminated sandstone facies*

Parallel laminated sandstone with intermittent mud laminae defines this facies (figure 5i). The average thickness of the facies is 20 cm. The facies exhibits vertical variations in lamina thickness (ca. 2 cm for sand lamina and 0.3 cm for mud lamina) (figure 5i). However, limited exposure does not permit the measurement of the thickness of sufficient numbers of laminae.

Interpretation: The presence of a thin lag between the Rohtas Limestone and the sandstone unit possibly represents a transgressive lag (Catuneanu 2006; Mandal *et al.* 2016). The presence of the transgressive lag along the boundary of the Rohtas Limestone and this sandstone indicates a fresh episode of sedimentation after the completion of the Lower Vindhyan sedimentation. The internal structures of sandstone, cyclicity in laminae thickness and high concentration of mud within all the constituting facies of the Facies association I indicate the tide-dominated depositional setting. The bed-load movement under the influence of dominant unidirectional current during the tidal regime is inferred. The alternations between the thick and thin foresets strongly support tidal actions. Bipolar and bimodal palaeocurrent directions (figure 5f) of herringbone patterned cross-stratified sandstone facies corroborates tidal actions (Visser 1980; De Boer *et al.* 1989; Bose *et al.* 1997). The presence of double mud drapes within this facies (figure 5g) indicates a subtidal environment (Visser 1980; Bose *et al.* 1997; Eriksson and Simpson 2004; Kohsiek and Terwindt 1981). The larger cycle, measured from alternating thick–thin laminae (figure 5b), is very much compatible with the lunar bi-monthly (spring to spring) cycle. This can readily be attributed to semidiurnal tides. The intra-set cyclic variations along with grain size indicate repeated waxing and waning of the water flow. In contrast to the bidirectional palaeocurrent pattern, alternating thick–thin tabular cross-stratified sandstone facies (facies 4.1.1) is unidirectional (figure 5c), indicating flow reversal during the abandoning phase of the tidal sand-waves (Nio and Yang 1991; Bose *et al.* 1997). In some places, mud laminae within the constituting facies are very thick (figure 5c). Such thick mud drapes in between the sand layers rarely form at any stage of the tidal cycle (McCave 1985; Chakraborty and Bose 1990). However, thick mud can be introduced to any tidal system from the outside by a process which is able to disperse mud in a suspension load from the shoreline environments, possibly by a super-storm event (Allen 1988; Chakraborty and Bose 1990). High-suspended sediment concentration may lead to the deposition of a thick mud layer during the neap period as well (Schieber 1986).

4.2 *Facies association II*

This association occasionally interferes with Facies association I. However, Facies association II, characteristically contains less mud compared to Facies association I. Facies association II primarily consists of coarse- to fine-grained sandstone. Five facies comprising Facies association II are discussed as follows:

4.2.1 *Conglomerate facies*

This facies occurs locally and is characterised by a matrix-supported conglomerate unit having a wedge-shaped geometry with a maximum thickness of $\sim$40 cm. The base of the facies is invariably sharp and scoured (figure 6a). The compositions of clasts include chertified limestone, vein quartz and sandstone (figure 6a and b). The maximum size of the clasts is 11 cm. The interstitial spaces between the clasts of the conglomerate are filled with a coarse-grained sandy matrix (figure 6a). This conglomerate facies often grades into a massive sandstone laterally and vertically (figure 6a).

4.2.2 *Massive sandstone facies*

This facies is characterised by massive, coarse- to medium-grained sandstone beds (thickness of the

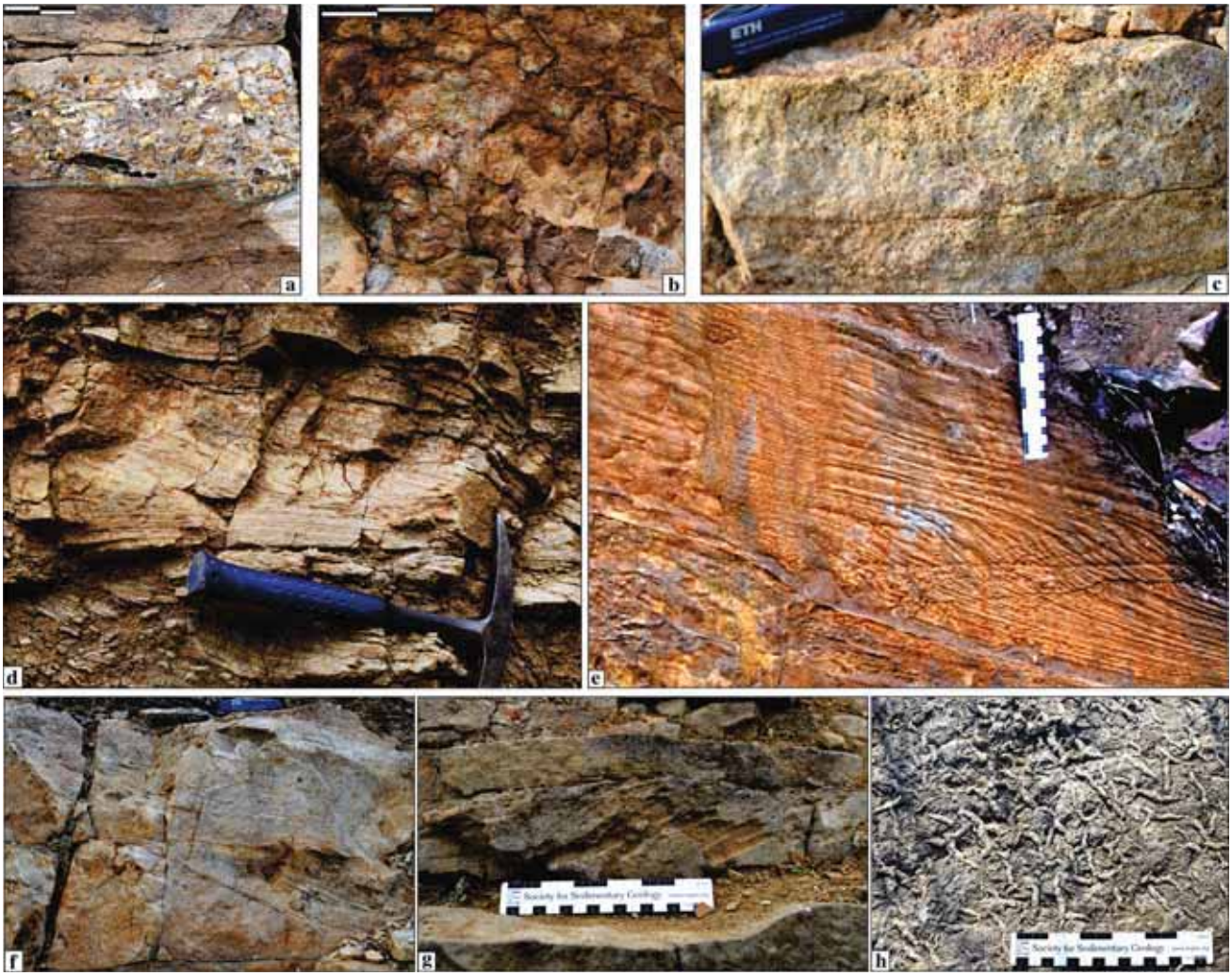

Figure 6. Facies association II; conglomerate facies (**a**, bar length 10 cm). Note the scoured base (marked by dotted lines) and upward gradation into massive sandstone. Sand clasts on the bedding plane surface (**b**, bar length 15 cm). Massive sandstone facies (**c**, length of knife 8 cm). The transition from planar to cross-lamination (**d**, hammer length 35 cm). Brink point maintaining the same level from the base within cross-stratification, massive sandstone facies (**e**, scale length 15 cm). Amalgamated cross-stratified facies (**f**, length of knife 8 cm). Hummocky cross-stratified facies (**g**, scale length 15 cm). Syneresis cracks on the bedding surface (**h**, scale length 15 cm).

facies is ∼20 cm) (figure 6c). The base of the facies is sharp than its top. Gutters, bipolar prod marks and local flutes are present at the sole of this facies. The massive beds often grade upward into planar laminated beds followed by cross-stratifications (figure 6d). The overall grain size of the facies decreases upward. Mud clasts are common at the base of the massive beds as well as along the cross-stratifications. The style of cross-stratification within a set changes laterally but non-cyclically. The brink point of the cross-stratifications maintains nearly the same distance from the base (figure 6e). The top of the sandstone beds is invariably wave-rippled (figure 4b). The ripple crests are straight in nature, having local bifurcations, although discernible asymmetry is common in their profiles.

4.2.3 *Tabular cross-stratified amalgamated sandstone facies*

This facies is characterised by amalgamated sandstone beds (figure 6f). The maximum thickness of the individual bed is ca. 32 cm but amalgamation may contribute to a thickness up to 1 m. Internal tabular cross-stratifications define the amalgamated sand beds (figure 6f). The palaeocurrent direction measured from these tabular cross-strata is directed towards the WSW direction (figure 4b). It is commonly associated with massive to feebly graded sandstone facies and hummocky cross-stratified sandstone facies (figure 4b). The bases of the facies are sharp while their tops are gradational with the occasional presence of wave-ripple laminations.

4.2.4 *Hummocky cross-stratified sandstone facies*

This facies is characteristically medium- to fine-grained, moderately sorted sandstone with broadly lenticular to tabular beds and convex-up tops (figure 6g). It is overlain by wave-ripple laminated facies (figure 4b) with less sharp contact. Hummocks and swales are frequently observed with the maximum height and wavelength ca. 8 and 35 cm, respectively. Bases of such beds generally replicate the underlying bed surface. Hence the bases are sharp but non-erosional, whereas the top of the beds is less sharp. This facies is commonly associated with the top part of the massive sandstone facies. Overall normal gradation is observed within the facies.

4.2.5 *Wave-ripple laminated sandstone facies*

This wave-ripple laminated sandstone facies generally overlies the top of the preceding facies. Ripple crests are straight and show bifurcations on the bedding plane. Syneresis cracks are abundantly present on the bed surfaces of these beds at different levels (figure 6h). Overall orientations of these cracks are fairly consistent but vary widely between beds (Pratt 2002).

Interpretation: The stacking pattern of beds within the facies of this association reveals occasional interruptions by high-energy events like storms within a tide-dominated environment. The massive sandstone facies indicates rapid dumping of the sediments. The massive character and absence of normal grading indicate deposition from short-lived, high-density flows. The high rate of sedimentation prevents the sorting process (Kneller and Branney 1995; Magalhães *et al.* 2015). The vertical and lateral transitions of conglomerate facies to massive sandstone indicate the deposition of both the component from a single flow. The scoured base of the conglomerate beds (figure 6a) at places indicates the presence of turbulence within the flow. The flow must have enough capacity to pick-up chertified limestone clasts from the topmost part of the Rohtas Limestone. The occurrence of amalgamated-sandstone beds within Facies association II, juxtaposed one above the other suggests the rapid recurrence of event flow, possibly storm surges, in a high-flow regime (Sarkar *et al.* 2004). The individual sandstone bed comprising amalgamated-sandstone facies indicates the product of a single depositional continuum over a relatively short time. A sharp irregular base with sole features also supports the high-energy events responsible for the deposition of the beds and the supercritical nature of the initial flow (Sarkar *et al.* 2012). The cross-stratification having brink points at the same height from the base suggests the high rate of sand fall-out from suspension possibly during the periods of a heavy storm. The steady upward decline in both grain-size and flow regime suggests a gradual waning of the high-energy events (Bose and Sarkar 1991). Preserved-wave ripple forms on the bedding surface and hummocky cross-stratified sandstone facies reflect deposition under the influence of the oscillatory flow, possibly during storm surges. Asymmetry in the ripple profiles indicates the simultaneous presence of a tractive force within the flow. Deposition from storm-generated combined, wave-cum-current, flow is thus inferred. Syneresis cracks present on the bed-surfaces of wave-ripple laminated sandstone facies possibly originate through the dewatering of the sandy beds due to the rapid deposition of the overlying sediment (Kidder 1990). Increased pore-water pressure because of storm wave action (Cowan and James 1992; Harazim *et al.* 2013; McMahon *et al.* 2017) may be responsible for the generation of syneresis cracks.

5. Discussion

The Rohtas Limestone is the topmost unit of the Lower Vindhyan succession. The limestone is overlain by laterally persistent sandstone in the studied stretch of the Son valley (figures 3 and 7). The sandstone is deposited on an undulating surface over a transgressive lag formed on the top surface of the Rohtas Limestone. The majority of the clasts are present within the lag derived from the Rohtas Limestone. The majority of the limeclasts are chertified. The topmost part of the Rohtas Limestone is also chertified at places. The degree of chertification also varies laterally to a remarkable extent. The chertified layers thus often appear to have irregular geometry and boundaries difficult to trace. Often they appear laterally discontinuous. Only exposure or near-exposure on the Earth's surface can account for this much abundance of silica during post-depositional alteration or weathering of the limestone. It is likely that part of the Rohtas Limestone was exposed for a long period of time which helps chertification (Kolodny *et al.* 1980). However, the transgressive lag indicates a fresh sedimentation event. The sedimentation started on a tide-dominated shelf. The

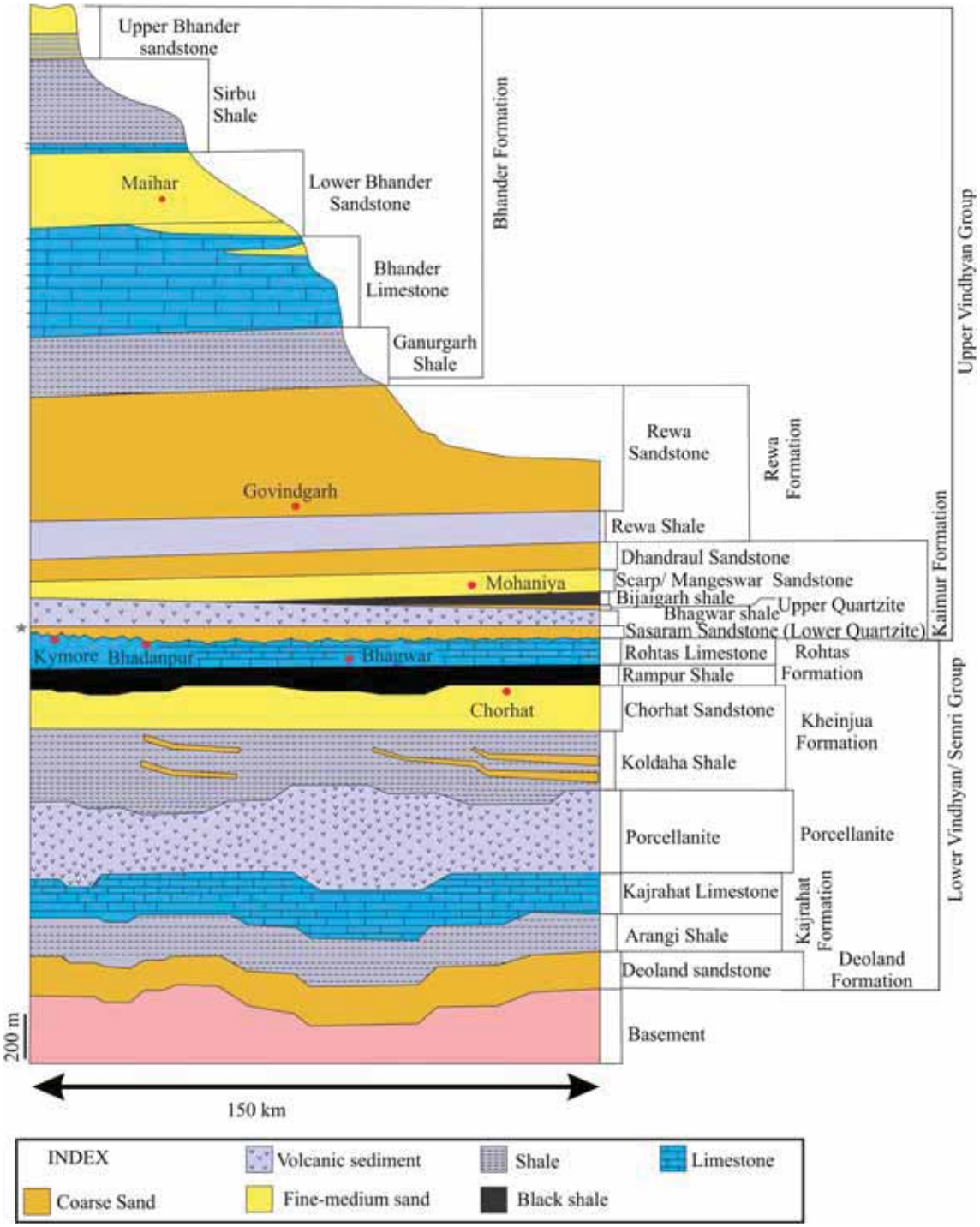

Figure 7. Stratigraphic column of the Vindhyan Supergroup present in the Son valley, central India (modified after Chakraborty 2006). Note the laterally persistent sandstone unit present above the Rohtas Limestone with an erosional surface in-between, traced from Mohaniya to Kymore.

presence of thick–thin alternation, double mud drape layers, herringbone cross-stratification, reactivation surface and frequently mud lamina within the cross-strata bear tell-tale evidence of tide domination. This tide-dominated environment intervened by storm is evidenced by the presence of hummocky cross-stratification, an amalgamation of sandstone beds and conglomerates/massive beds with sole features. The presence of numerous sand-clasts within the Facies association II supports the influence of microbiota that turned sand into a cohesive sediment (Sarkar *et al.* 2014, 2018). The vertical transition of the facies assemblages rules out any major palaeogeographic shift. Some of

them indicate clear evidence of subtidal deposition while a shallow marine depositional environment can be inferred from the sandstone unit in general. This sandstone unit is gradationally overlain by a shale unit known as Bhagwar Shale, also laterally persistent over the studied area (figure 7).

The boundary between the Lower and the Upper Vindhyan should be placed below the sandstone unit that indicates a change from a carbonate depositional system of Rohtas Limestone to a siliciclastic regime. The presence of a transgressive lag, consisting of pebbles of chertified limestone supports the initiation of a sedimentation event after a considerable gap. This sandstone deposited above the Rohtas Limestone is likely to be the equivalent of the Sasaram Sandstone (Lower Quartzite Member of the Kaimur Formation) reported from the Bundelkhand sector of the Vindhyan basin (Chakraborty 2006; Chakraborty *et al.* 2010). The depositional milieu of the newly studied sandstone resembles that of Sasaram Sandstone (Chakraborty and Bose 1990). After considering the detailed study in this part of the Son valley sector, it seems the boundary between the Upper and the Lower Vindhyan has not been placed properly (figures 2 and 7). Rather it will be more logical to put the boundary between the same at the base of the newly discovered sandstone which is the equivalent of the Sasaram Sandstone (Lower Quartzite).

6. Conclusions

1. The two-tier stratigraphic subdivision of the Vindhyan Supergroup, namely, the Lower and Upper Vindhyan is well established in the literature. The unconformity separating the Lower and Upper Vindhyan is placed above the Rohtas Limestone Member in the Bundelkhand sector. However, in the Son valley sector, it is placed above the Bhagwar Shale, a sandstone–shale heterolithic unit. Our study, therefore, contradicts the existing view regarding a gradational transition between the Rohtas Limestone and the overlying Bhagwar Shale.
2. Revisiting contact relationship between the Bhagwar Shale and Rohtas Limestone with the employment of process-based facies analysis, the present study documents a ∼12 m thick laterally persistent sandstone unit, hitherto undescribed, directly above the Rohtas Limestone with a sharp, erosional contact. The sandstone gradationally passes upward to the *sensu-stricto* Bhagwar Shale.
3. The presence of a transgressive lag dominantly consists of chertified lime clasts picked up from the long-exposed Rohtas Limestone surface, at the basal part of the sandstone unit bears telltale evidence for the initiation of a new sedimentation regime with transgression on the unconformable surface.
4. From the interpretation of depositional processes, a shallow-marine, subtidal environment is suggested for the sandstone unit. Possibly a tide-dominated shelf condition developed with transgression, occasionally intervened by storm. Similar sedimentation history also recorded from the Sasaram Sandstone (i.e., Lower Quartzite member of the Kaimur Formation) that overlies the Rohtas Limestone in the Bundelkhand sector.
5. The process-based appraisal indicates that sedimentation starts with a laterally persistent sandstone above the unconformable surface of Rohtas Limestone. The sandstone, in turn, gives way upward to the Bhagwar Shale.
6. The contact between the Lower and the Upper Vindhyan in the Son valley should be placed below the sandstone described in this work and not above the Bhagwar Shale.

Acknowledgements

The authors acknowledge the infrastructure support provided by their host institutes. SM acknowledges the UGC; AC, the DST Inspire Faculty programme; IM, the CSIR for providing a research grant and SS, the CAS (Phase VI), Department of Geological Sciences, JU for funding the fieldwork.

References

Allen J R L 1988 Reworking of muddy intertidal sediments in the Sevem Estuary, southwestern UK – a preliminary survey; *Sedim. Geol.* **50** 1–23.

Auden J B 1933 Vindhyan sedimentation in Son valley, Mirzapur District; *Geol. Surv. India Memoir* **62** 141–250.

Banerjee I 1974 Barrier coastline sedimentation model and the Vindhyan example; In: *Contribution to earth and planetary sciences* (ed.) De A, *Quart. J. Geol. Min. Met. Soc. India* **62** 101–127.

Banerjee S, Bhattacharya S K and Sarkar S 2006 Carbon and oxygen compositions of the carbonate facies in the

Vindhyan Supergroup, central India; *J. Earth Syst. Sci.* **115** 113–134.

Bengtson S, Belivanova V, Rasmussen B and Whitehouse M 2009 The controversial 'Cambrian' fossils of the Vindhyan are real but more than a billion years older; *Proc. Nat. Acad. Sci. USA* **106** 7729–7734.

Bengston S, Sallstedt T, Belivanova V and Whitehouse M 2017 Three-dimensional preservation of cellular and subcellular structures 1.6 billion-year-old crowd-group red algae; *PLoS Biol.,* https://doi.org/10.1371/journal.pbio.2000735.

Bhattacharyya A 1996 *Recent advances in Vindhyan geology;* Geol. Soc. India, 331p.

Bhattacharyya A and Morad S 1993 Proterozoic braided ephemeral fluvial deposits: An example from the Dhandraul sandstone formation of the Kaimur Group, Son Valley, central India; *Sedim. Geol.* **84** 101–114.

Bickford M E, Mishra M, Mueller P A, Kamenov G D, Schieber J and Basu A 2017 U–Pb age and Hf Isotopic compositions of magmatic zircons from a rhyolite flow in the Porcellanite formation in the Vindhyan Supergroup, Son Valley (India): Implications for its tectonic significance; *J. Geol.* **125** 367–379.

Bose P K and Sarkar S 1991 Basinal autoclastic mass flow regime in the Precambrian Chanda limestone formation, Adilabad, India; *Sedim. Geol.* **73** 299–315.

Bose P K and Chakraborty P 1994 Marine to fluvial transition: Proterozoic upper Rewa Sandstone, Maihar, India; *Sedim. Geol.* **89** 285–302.

Bose P K, Banerjee S and Sarkar S 1997 Slope-controlled seismic deformation and tectonic framework of deposition: Koldaha Shale, India; *Tectonophys.* **269** 151–169.

Bose P K, Chakraborty S and Sarkar S 1999 Recognition of ancient eolian longitudinal dunes; a case study in upper Bhander Sandstone, Son valley, India; *Int. J. Sedim. Res.* **69** 86–95.

Bose P K, Sarkar S, Chakrabarty S and Banerjee S 2001 Overview of Meso- to Neoproterozoic evolution of Vindhyan Basin, central India; *Sedim. Geol.* **141–142** 395–419.

Bose P K, Sarkar S, Das N G, Banerjee S, Mandal A and Chakraborty N 2015 Proterozoic Vindhyan Basin: Configuration and evolution; In: *Precambrian basins of India: Stratigraphic and tectonic context* (eds) Mazumder R and Eriksson P G, *Geol. Soc. London Memoir* **43**(**1**) 85–102.

Catuneanu O 2006 *Principles of sequence stratigraphy*; Elsevier, Amsterdam, 375p.

Chakraborty C 1993 Morphology, internal structure and mechanics of small longitudinal (seif) dune in an Aeolian horizon of the Proterozoic Dhandraul Quartzite, India; *Sedimentology* **40** 79–85.

Chakraborty C 1995 Gutter casts from the Proterozoic Bijaygarh Shale formation, India: Their implication for storm-induced circulation in shelf settings; *Geol. J.* **30** 69–78.

Chakraborty C 2006 Proterozoic intracontinental basin: The Vindhyan example; *J. Earth Syst. Sci.* **115** 3–22.

Chakraborty C and Bose P K 1990 Internal structures of sand waves in a tide-storm interactive system: Proterozoic lower quartzite formation, India; *Sedim. Geol.* **67** 133–142.

Chakraborty T and Chaudhuri A K 1990 Stratigraphy of Proterozoic Rewa group and palaeogeography of the Vindhyan Basin in central India during Rewa sedimentation; *J. Geol. Soc. India* **36** 383–402.

Chakraborty C and Bose P K 1992a Rhythmic shelf storm beds: Proterozoic Kaimur formation, India; *Sedim. Geol.* **77** 259–268.

Chakraborty C and Bose P K 1992b Ripple/dune to upper stage plane bed transition: Some observations from the ancient record; *Geol. J.* **27** 349–359.

Chakraborty P P, Banerjee S, Das N G, Sarkar S and Bose P K 1996 Volcaniclastics and their sedimentological bearing in Proterozoic Kaimur and Rewa Groups in central India; *Mem. Geol. Soc. India* **96** 59–75.

Chakraborty T and Chakraborty C 2001 Eolian-aqueous interactions in the development of a Proterozoic sand sheet: Shikaoda formation, Hosangabad, India; *J. Sedim. Res.* **71** 107–117.

Chakraborty P P, Dey S and Mohanty S P 2010 Proterozoic platform sequences of Peninsular India: Implications towards basin evolution and supercontinent assembly; *J. Asian Earth Sci.* **39** 589–607.

Chakraborty P P, Sarkar S and Patranabis-Deb S 2012 Tectonics and sedimentation of Proterozoic Basins of Peninsular India; *Proc. Indian Nat. Sci. Acad.* **78** 393–400.

Chanda S K and Bhattacharyya A 1982 Vindhyan sedimentation and palaeogrography; post-Auden development; In: *Geology of Vindhyachal* (eds) Valdiya K S, Bhatia S B and Gaur V K, Hind. Publ. Corp. (India), Delhi, pp. 88–101.

Cowan C A and James N P 1992 Diastasis cracks: Mechanically generated synaeresis-like cracks in upper Cambrian shallow water oolite and ribbon carbonates; *Sedimentology* **39** 1101–1118.

De Boer P L, Oost A P and Visser M J 1989 The diurnal inequality of the tide as parameter for recognizing tidal influences; *J. Sediment. Res.* **59** 912–921.

Eriksson K A and Simpson E L 2004 Precambrian tidalites: Recognition and significance; In: *Tempos and events in Precambrian time: Amsterdam* (ed.) Eriksson P G, Elsevier Science, pp. 631–642.

Gilleaudeau G J, Sahoo S P, Kah L C, Henderson M A and Kaufman J 2018 Proterozoic carbonates of the Vindhyan Basin, India: Chemostratigraphy and diagenesis; *Gondwana Res.* **57** 10–25.

Gopalan K, Kumar A, Kumar S and Vijayagopal B 2013 Depositional history of the upper Vindhyan succession, central India: Time constraints from Pb–Pb isochron ages of its carbonate components; *Precamb. Res.* **233** 108–117.

Harazim D, Callow R H and McIlroy D 2013 Microbial mats implicated in the generation of intrastratal shrinkage ('synaeresis') cracks.; *Sedimentology* **60** 1621–1638.

Kidder D L 1990 Facies-controlled shrinkage-crack assemblages in middle Proterozoic mudstones from Montana, USA; *Sedimentology* **37** 943–951.

Kneller B C and Branney M J 1995 Sustained high-density turbidity currents and the deposition of thick massive sands; *Sedimentalogy* **42** 607–616.

Kohsiek L H M and Terwindt I H I 1981 Characteristics of foreset and topset bedding in megaripples related to hydrodynamic conditions on an intertidal shoal; In: *Holocene marine sedimentation in the North Sea basin* (eds) Nio S D, Schllttenhelm R L E and Van Weering T J C E, *IAS Spec. Publ.* **5** 27–37.

Kolodny Y, Taraboulos A and Frieslander U 1980 Participation of fresh water in chert diagenesis: Evidence from

oxygen isotopes and boron a-track mapping; *Sedimentology* **27** 305–316.

Kumar S 1978a Stromatolites and environment of deposition of the Vindhyan Supergroup of Central India; *J. Palaeontol. Soc. India* **21–22** 33–43.

Kumar S 1978b Sedimentaries of the zone of Badolisera and the Vindhyan Supergroup, Uttar Pradesh – A reappraisal of correlation; *J. Palaeontol. Soc. India* **21–22** 96–101.

Kumar S and Sharma M 2011 Vindhyan Basin, Son Valley Area, central India; The Palaeol. Soc. of India, Field Guide, 121p.

Magalhães A J C, Gabaglia G P, Scherer C M S, Ballico M B, Guadagnia F, Bento Freeire E, Silva Born L R and Octavian C 2015 Sequence hierarchy in a Mesoproterozoic interior sag basin: From basin fill to reservoir scale, the Tombador formation, Chapada Diamantina Basin, Brazil; *Basin Res.* **28** 393–342.

Malone S J, Meert J G, Banerjee D M, Pandit M K, Tamrat E, Kamevon G D, Pradhan V R and Sohl L E 2008 Paleomagnetism and detrital zircon geochronology of the upper Vindhyan sequence, Son valley and Rajasthan, India: A ca. 1000 Ma closure age for the Puranabasin? *Precamb. Res.* **164** 137–159.

Mandal A, Koner A, Sarkar S, Tawfik H A, Chakraborty N, Bhakta S and Bose P K 2016 Physico-chemical tuning of palaeogeographic shifts: Bhuj formation, Kutch, India; *Mar. Pet. Geol.* **78** 474–492.

McCave I N 1985 Recent shelf elastic sediments; In: *Sedimentology: Recent developments and applied aspects* (eds) Brenchley P J and Williams B P S, *Geol. Soc. of London, Spec. Publ.* **18** 49–65.

McMahon S, Hood A V S and McIlroy D 2017 The origin and occurrence of subaqueous sedimentary cracks; In: *Earth system evolution and early life: A celebration of the work of Martin Brasier* (eds) Brasier A T, McIlroy D and McLoughlin N, *Geol. Soc. London, Spec. Publ.* **448** 285–309.

McMenamin D S, Kumar S and Awramik S M 1983 Microbial fossils from the Kheinjua Formation, Middle Proterozoic Semri Group (lower Vindhyan) Son valley area, Central India; *Precamb. Res.* **21** 247–271.

Mishra M, Bickford M E and Basu A 2018 U-Pb Age and chemical composition of an Ash Bed in the Chopan Porcellanite Formation, Vindhyan Supergroup, India; *J. Geol.* **126**(**5**) 553–560.

Naqvi S M and Rogers J J W 1987 *Precambrian geology of India*; Clarendon Press; Oxford Univ. Press, New York, Oxford, 233p.

Nio S D and Yang C S 1991 Diagnostic attributes of clastic tidal deposits: A review; In: *Clastic tidal sedimentology: Calgary* (eds) Smith D G, Zaitlin B A, Reinson G E and Rahmani R A, *Can. Soc. Pet. Geol.*, pp. 3–27.

Paikaray S, Banerjee S and Mukherji S 2008 Geochemistry of shales from the Paleoproterozoic to Neoproterozoic Vindhyan Supergroup: Implications on provenance tectonics and paleoweathering; *J. Asian Earth Sci.* **32** 34–48.

Pati J K, Reimold W U, Koeberl C and Pati P 2008 The Dhala structure, Bundhelkhand craton, central India-eroded remnant of large Paleoproterozoic impact structure; *Meteor. Planet. Sci.* **43**(**8**) 1383–1398.

Prasad B and Verma K K 1991 Vindhyam basin: A review; In: *Sedimetary basin of India: Tectonics context* (eds) Tandon S K, Pant C C and Casshyap S M, Gyanodaya Prakashan, Nainital, India, pp. 50–62.

Pratt B R 2002 Syneresis cracks: Subaqueous shrinkage in argillaceous sediments caused by earthquake-induced dewatering; *Sedim. Geol.* **117**(**1**) 1–10.

Rai V, Shukla M and Gautam R 1997 Discovery of carbonaceous megafossils (Chauria–Tawuiaassenblagge) from the Neoproterozoic Vindhyan succession (Rewa Group), Allahabad–Rewa area, India; *Curr. Sci.* **73** 783–788.

Rao K S and Neelakantam S 1978 Stratigraphy and sedimentation of Vindhyans in parts of Son valley area, Madhya Pradesh; *Rec. Geol. Surv. India* **110** 180–193.

Rasmussen B, Bose P K, Sarkar S, Banerjee S, Fletcher I R and Mcnaughton N J 2002 1.6 ga U–Pb zircon age for the Chorhat Sandstone, lower Vindhyan, India: Possible implications for early evolution of animals; *Geology* **30** 103–106.

Ray J S, Martin M W, Veizer J and Bowring S A 2002 U–Pb zircon dating and Sr isotope systematic of Vindhyan Supergroup, India; *Geology* **30** 131–134.

Ray J S, Veizer J and Davis W J 2003 C, O, Sr and Pb isotope systematic of carbonate sequences of the Vindhyan Supergroup, India: Age, diagenesis, correlations and implication for global events; *Precamb. Res.* **121** 103–140.

Raza M, Dayal A M, Khan A, Bhardwaj V R and Rais S 2010 Geochemistry of lower Vindhyan clastic sedimentary rocks of northwestern Indian shield: Implications for composition and weathering history of Proterozoic continental crust; *J. Asian Earth Sci.* **39** 51–61.

Rouse R 1961 *Fluid mechanics for hydralic engineers*; Dover, New York.

Sallstedt T, Bengtson S, Broman C, Crill P M and Canfield D E 2018 Evidence of oxygenic phototrophy in ancient phosphatic stromatolites from the Paleoproterozoic Vindhyan and Aravalli Supergroups, India; *Geobiology* **16** 139–159.

Sarangi S, Gopalan K and Kumar S 2004 Pb–Pb of earliest magascopic, eukaryotic alga bearing Rohtas formation, Vindhyan Supergroup, India: Implication for Precambrian atmospheric oxygen evolution; *Precamb. Res.* **132** 107–121.

Sarkar S, Chakraborty P P and Bose P K 1996 Proterozoic lakheri limestone, central India; facies, paleogeography and physiography; *Mem. Geol. Soc. India* **36** 5–26.

Sarkar S, Banerjee S, Chakarborty S and Bose P K 2002a Shelf storm flow dynamics: Insight from the Mesoproterozoic Rampur Shale, Central India; *Sedim. Geol.* **147** 89–104.

Sarkar S, Chakarborty S, Banerjee S and Bose P K 2002b Facies sequence and cryptic imprint of sag tectonics in the late Proterozoic Sirbu Shale, Central Shale; *IAS Spec. Publ.* **33** 369–381.

Sarkar S, Eriksson P G and Chakraborty S 2004 Epeiric sea formation on Neoproterozoic supercontinent break-up: A distinctive signature in coastal storm bed amalgamation; *Gondwana Res.* **7**(**2**) 313–322.

Sarkar S, Banerjee S, Samanta P and Jeevankumar S 2006 Microbial mat-induced sedimentary structures in siliciclastic sediments: Examples from the 1.6 Ga Chorhat Sandstone, Vindhyan Supergroup, MP, India; *J. Earth Syst. Sci.* **115** 49–60.

Sarkar S, Banerjee S, Mukhopadhyay S and Bose P K 2012 Stratigraphic architecture of the Sonia Fluvial interval, India in its Precambrian context; *Precamb. Res.* **214–215** 210–226.

Sarkar S, Banerjee S, Samanta P, Chakraborty N, Chakraborty P P, Mukhopadhyay S and Singh A K 2014 Microbial mat records in siliciclastic rocks: Examples from four Indian Proterozoic basins and their modern equivalents in Gulf of Cambay; *J. Asian Earth Sci.* **91** 362–377.

Sarkar S, Choudhuri A, Mandal S and Bose P K 2018 Flat pebbles and their edge-wise fabric in relation to 2-D microbial mat; *Geol. J.,* https://doi.org/10.1002/gj.3312.

Sastry M V A and Moitra A K 1984 Vindhyan stratigraphy: A review; *Geol. Surv. India Memoir* **116** 109–148.

Schieber J 1986 The possible role of benthic microbial mats during the formation of carbonaceous shales in shallow Mid-Proterozoic basins; *Sedimentology* **33** 521–536.

Schieber J, Sur S and Banerjee S 2007 Benthic microbial mats in black shale units from Vindhyan supergroup, Middle Proterozoic of India: The challenges of recognizing the genuine article; In: *Atlas of microbial mats features preserved within the clastic rock record* (eds) Schieber J, Bose P K, Eriksson P G, Banerjee S, Sarkar S, Altermann W and Catunneau O, Elsevier, pp. 189–197.

Seilacher A, Bose P K and Pflüger F 1998 Triploblastic animals more than 1 billion years ago: Trace fossil evidence from India; *Science* **282** 80–82.

Singh L B 1973 Depositional environment of the Vindhyan sediments in the Son valley area; In: Recent Researches in Geology Hindu. Pub. Corp., New Delhi, pp. 146–152.

Srivastava A P and Rajagopalan G 1988 F–T ages of Vindhyan glauconitic sandstone beds exposed around Rawatbhata area, Rajasthan; *J. Geol. Soc. India* **32** 527–529.

Tripathy G S and Singh S K 2015 Re–Os depositional age for black shale from the Kaimur Group, upper Vindhyan, India; *Chem. Geol.* **413** 63–72.

Valdiya K S 2010 The Making of India Geodynamics Evolution; pp. 191–193.

Visser M J 1980 Neap-spring cycles reflected in Holocene subtidal large-scale bedform deposits: A preliminary note; *Geology* **8** 543–546.

Corresponding editor: N V Chalapathi Rao